^{186,187,188}Os(n,γ) cross sections and galactic nucleosynthesis

R. R. Winters,* R. L. Macklin, and J. Halperin
Physics Division, Oak Ridge National Laboratory, Oak Ridge, Tennessee 37830
(Received 9 July 1979)

The ^{186,187,188}Os(n,γ) cross sections were measured over the incident neutron energy range 2.6–800 keV. Optimized statistical model fits to the average cross sections were made employing estimates of the ^{186}Os, ^{187}Os, and ^{188}Os p-wave strength functions 0.29×10^{-4}, 0.45×10^{-4}, and 0.33×10^{-4}, respectively, d-wave strength functions 1.3×10^{-4}, 4.0×10^{-4}, and 1.5×10^{-4}, respectively, and gamma ray strength functions $(\bar{\Gamma}_\gamma/D_0)$ 26.8×10^{-4}, 176×10^{-4}, and 20.8×10^{-4}, respectively. A lower bound for the ^{187}Os neutron inelastic cross section is estimated as 0.25(20) b at 30 keV. The Maxwellian-averaged capture cross sections are presented as a function of temperature. The ratio of 30 keV Maxwellian-averaged cross sections $\langle\sigma_\gamma(186)\rangle/\langle\sigma_\gamma(187)\rangle = 0.504(17)$ is reported and the lack of agreement with earlier measurements of this ratio is discussed. The use of this cross section ratio in estimating, via the ^{187}Re-^{187}Os beta decay, the duration of galactic nucleosynthesis is discussed. The cross section ratio from this work yields an estimate of $10.4(25)\times10^9$ yr for the duration of galactic nucleosynthesis, a result higher than but still consistent with the estimate $7(2)\times10^9$ yr derived from U/Th decay.

[NUCLEAR REACTIONS Neutron capture, cross section, inelastic cross section, strength functions, nucleosynthesis, Maxwellian-averaged cross section.]

INTRODUCTION

As first pointed out by Clayton,[1] the ^{187}Re→^{187}Os beta decay represents an isobaric pair uniquely well suited for use as a chronometer of nucleosynthesis. However, use of this chronometer has led to estimates for the duration of nucleosynthesis approximately a factor of two larger than that using the uranium-thorium chronometer. Conrad and Zeh,[2] Talbot,[3] and Woosley and Fowler[4] have extensively discussed the difficulties inherent in the application of the Re-Os decay. As these references make clear, exploitation of the rhenium beta decay as a probe of the epoch of nucleosynthesis depends on careful remeasurements of the beta decay rate, measurement of the inelastic neutron cross section to the first excited state in ^{187}Os, and remeasurement of the ^{186}Os and ^{187}Os capture cross sections to corroborate the only previous measurements[5,6] available. This paper describes measurements of the capture cross sections. The cross sections resulting from this work differ from those reported in Ref. 5 and 6. This has prompted a careful appraisal of the earlier work and now those cross sections have been revised in a direction toward agreement with our work. The resulting cross section uncertainties are small compared to uncertainties in the other parameters required for use of the Re-Os decay as a chronometer.

THE EXPERIMENTAL MEASUREMENTS

The neutron capture cross sections for the osmium isotopes 186, 187, and 188 were measured over the incident neutron energy range 2.6 to about 800 keV at the Oak Ridge Electron Linear Accelerator (ORELA). The accelerator was operated at 800 pulses/sec with an electron burst width of ≈8 nsec FWHM (full width at half maximum). The measurements were made at the 40 m station, flight path 7, capture facility[7] shown in Fig. 1. Neutron energy resolution width ranged from $\Delta E/E = 0.16\%$ at 2.5 keV to $\Delta E/E = 0.5\%$ at 800 keV FWHM. The neutron flux was monitored using a thin (0.5 mm) piece of ^{6}Li glass placed $\simeq\frac{1}{2}$ m upstream from the capturing sample in the neutron beam. The BF_3 neutron monitor shown in Fig. 1 was not used for this experiment. The neutron capture rate was measured by detecting the prompt γ rays associated with the deexcitation of the compound nucleus. A pair of fluorocarbon-based liquid scintillation detectors (labeled "Nonhydrogeneous" in Fig. 1) are symmetrically placed on either side of the capturing sample. This arrangement reduces effects of possible misalignment of the sample or neutron beam to less than 0.2%. The efficiency of the γ ray detectors is made independent of the capture γ ray cascade spectrum by pulse height weighting[8] each capture event (above a sharp 153-keV bias) detected in the fluorocarbon scintillators. The pulse height weighting results in an efficiency which is proportional to the total energy (binding plus kinetic energy) available from the compound nucleus deexcitation γ spectrum. The efficiency independence has been confirmed[9,10] (to $\simeq1\%$) for the 3.92-eV resonance in holmium, the 6.7-eV resonance in uranium-238, and the 5.19-eV resonance in silver. The normalization

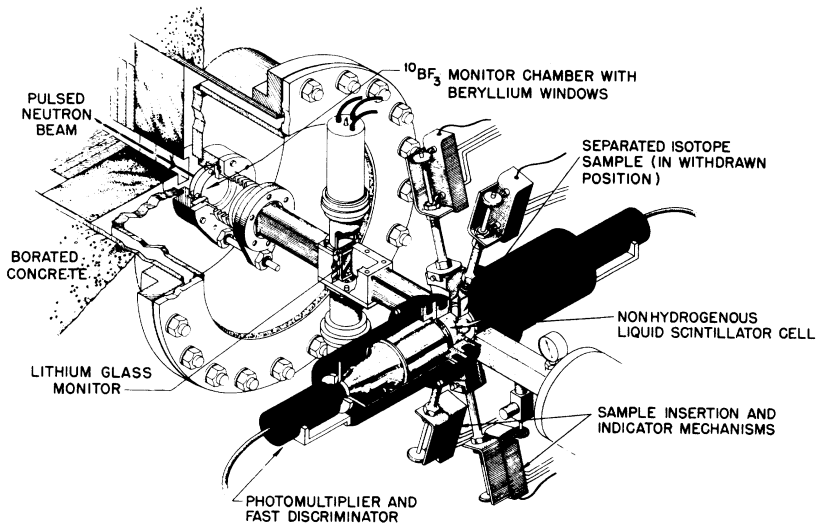

FIG. 1. The ORELA capture facility on flight path 7 at the 40 m flight path station.

of the calculated detection system efficiency is accomplished by saturation of the 4.9-eV resonance in (^{197}Au + n). For this gold resonance, the capture reaction dominates over elastic scattering. The gold sample used is sufficiently thick (0.0029 atoms/b) so that neutron transmission near the peak of the resonance is negligible, hence the capture yield per incident neutron flux is measured. The neutron escape probability (≈2.6%, primarily due to back scattering from the gold) was determined using a Monte Carlo calculation. Values of the detection efficiency normalization factor (TEDEFF) determined by saturating the 4.9-eV gold resonance are presented in Table I. The procedure for evaluating TEDEFF is described in greater detail by Macklin *et al.*[11]

The work described in this paper is based on two two-week accelerator operating cycles during which efficiency calibration runs and system stability checks were interspersed with the osmium capture cross section measurements. Results of periodic checks of the detection system gain sta-

TABLE I. Sequence of the ORELA Os(n,γ) experiments.

Run no.	Experiment	TEDEFF/Monitor comments
8050	Sat. 4.9-eV Au	1.0109(47)
8060	^{187}Os(n,γ)	26.1×10^6
8070	^{186}Os(n,γ)	30.0×10^6
	double source check	1.4% gain adjustment
8080	Sat. 4.9-eV Au	1.0122(46)
	double source check	no gain adjustment
8090	No sample	background measurement
8100	^{188}Os(n,γ)	25.1×10^6
	double source check	no gain adjustment
8110	^{187}Os(n,γ)	85.7×10^6
	double source check	no gain adjustment
	No beam	background measurement
8120	Sat. 4.9-eV Au	1.0094(39)
8140	^{186}Os(n,γ)	106 $\times 10^6$
	double source check	0.9% gain adjustment
8150	^{188}Os(n,γ)	37.5×10^6
8160	Sat. 4.9-eV Au	1.0072(45)
	double source check	no gain adjustment
8170	No sample	background measurement
	double source check	no gain adjustment

bility using a Pu-Be source (total energy detectors) and a ^{241}Am α source (flux monitor) are included in Table I. The total energy detector efficiency varies as the 1.387 power of the variation (relative to a reference value) of the gain. The entries in Table I suggest that the largest variation in efficiency observed during these experiments was ≈0.3%.

PRELIMINARY DATA ANALYSIS

The data rates for these measurements are much less than one event for each neutron burst and hence the time interval digitizer is operated on a one stop per neutron burst basis. This means that the clock dead time is dominant and the dead time corrections are easily calculable. The maximum dead time correction for the flux monitor was ≲2% and for the total energy detectors ≈8%, very nearly independent of the particular run. The accelerator-independent backgrounds are monitored during each run over the time of flight interval 900–951 μsec (≈11 eV), where the ^{10}B overlap filter is nearly black, and, as shown in Table I, were also monitored during a period when the accelerator was off. Near 2.5 keV, this background was ≈12% of the foreground for the second ^{186}Os and ^{187}Os runs, and was ≈20% for both of the (shorter) ^{188}Os runs. The accelerator-dependent, sample-independent background correction is conventionally found as the average of a number of long duration runs without a sample (corrected for the accelerator-independent background) and was 22% for the ^{186}Os runs, 13% for the ^{187}Os, and 36% for the ^{188}Os over the range 2.5–6.0 keV. The uncertainty deriving from this correction was estimated to be ≲5% of the correction. These two background corrections are relatively large, but a check on the precision with which they were performed is provided by the two no-sample runs. When the no-sample runs were corrected for these backgrounds, it was found that the resultant residues were zero within counting statistics. In order to retain as much shape information in the cross section data as possible, however, the residues were restored to the data after correction for each of the measured backgrounds. There is also a time-dependent sample-dependent background which is obtained from a ^{208}Pb long duration run and scaled via scattering cross section to the isotope of interest. This correction over the 2.5–6.0 keV range was ≈4% for the ^{186}Os runs, ≈2% for the ^{187}Os runs, and ≈7% for the ^{188}Os. The uncertainty propagated for the background corrections was the larger of the residues for the no-sample data or the statistical uncertainty propagated through the various background corrections. The resulting uncertainties for a 0.25-keV averaging interval centered at 2.75 keV were 1% of the corrected cross section for the ^{186}Os runs, 0.5% for ^{187}Os, and 1.6% for ^{188}Os. The small size of these uncertainty estimates is remarkable since the osmium samples were of much smaller mass (2 g for the 187 and 188 samples and 2.98 g for the 186 sample) than the 0.1 mole for which the ORELA capture facility was designed. In addition to the corrections for background effects, the raw data also were corrected for γ ray absorption in the Os samples. The attenuation was calculated for the ORELA capture facility geometry and for a typical capture cascade spectrum. The correction resulted in an approximately 10% enhancement of the observed capture yield nearly independently of the particular osmium sample. The uncertainty in this correction is assumed negligible.

The isotopic enrichments of the osmium samples are given in Table II. Corrections for the isotopic impurity contributions for the high resolution capture yield involve detailed knowledge of the sample thickness effects and hence of the total capture cross sections. Fortunately in this work, since it is the average capture cross sections which are of interest, only average sample thickness and isotopic impurity corrections are required. To effect these corrections the observed capture yields were averaged into energy bins of width large compared with the reported resonance spacings. Below 112 keV these bins were 0.250 keV wide, and hence contained tens of resonances. Above 100 keV, wider bins were used.

TABLE II. Isotopic composition (in atomic percent) of the osmium samples. Elemental impurities are <1.8% for the ^{186}Os sample, <1.2% for the ^{187}Os sample, and <0.04% for the ^{188}Os sample.

Enriched isotope	184	186	187	188	189	190	192
186	<0.02	78.39(15)	1.62(3)	5.07(5)	4.09(4)	5.15(5)	5.67(6)
187	<0.05	0.93(2)	70.38(15)	12.79(10)	5.28(5)	5.41(5)	5.26(5)
188	<0.05	0.13(3)	0.17(3)	94.47(20)	2.77(5)	1.42(4)	1.04(4)

The sample thickness correction factors were calculated using a modification, as described by Macklin,[12,13] of a procedure suggested by Dresner[14] which explicitly includes level fluctuation effects. Near 30 keV, the net corrections are 3% (^{186}Os), 6% (^{187}Os), and 2%(^{188}Os) and are predominantly due to multiple scattering. Near 100 keV the correction reaches 8% for all of the isotopes, then decreases slowly at still higher energies as the total scattering cross section drops and becomes more forward peaked. Below 30 keV, resonance self-protection is more significant for these sample thicknesses, balancing the multiple scattering effect near 20 keV for the even isotopes and near 3.1 keV for the odd isotope. At our lowest energies ($\simeq$3 keV) the resonance self-protection becomes particularly severe for the even isotopes with their higher peak total cross sections, reducing average capture per nucleus up to 37% compared with a sample of negligible thickness. Input parameters for these sample thickness correction calculations are the s-wave strength functions and level spacings for the even isotopes taken from the work of Vertebnyi,[15] the p-wave strength functions estimated from those reported[16] for other nuclei in this mass region, and the nuclear level spacings for ^{187}Os taken from the work by Stolovy *et al.*[17]

The correction for isotopic impurity contributions to the observed capture yield for a sample highly enriched in one major isotope takes advantage of the linearity of each isotopic contribution to the total observed γ energy yield for any isotopically enriched sample. Thus the observed capture yield for the sample enriched in isotope $i=186$, 187,188 can be written

$$Y_i(E)=C_{ij}Y'_j(E), \quad j=186,187,188,189,190,192 \quad (1)$$

where $Y'_j(E)$ is the yield from a sample of 100% enrichment in the jth major isotope. The composition matrix C has as elements the fractional abundances (Table II) of the various isotopes present in a sample enriched in a given isotope. The capture yields $Y'_j(E)$ from isotopically pure samples are found by simply inverting the composition matrix

$$Y'_j(E)=C_{ji}^{-1}Y_i(E). \quad (2)$$

Since only samples enriched in ^{186}Os, ^{187}Os, and ^{188}Os were used in this work, estimates for the capture cross sections for the minor impurities ^{189}Os, ^{190}Os, and ^{192}Os were required to correct for these small but nonnegligible contributions. Browne and Berman[18] have measured these cross sections and generously provided us with ratios of these three cross sections to their ^{188}Os cross section. The use of ratios reduces the propagation of systematic errors from the measurement of Browne and Berman to the present work. The sensitivity of the isotopic unscrambling to uncertainties in the assumed minor impurity cross sections was examined by performing the unscrambling for a number of assumed minor impurity cross sections. One such assumption was to treat the 189 as 187, and the 190 and 192 as 186. This approximation led to capture yields differing not more than 12% from those using Browne's ratios, giving, for example, differences of 9% (186), 6% (187), and 9% (188) near 30 keV. These are relatively small effects considering that treating the 189 as 187 underestimates that capture yield by a factor of 1.8. This insensitivity to the effects of minor impurity contributions is due to the nearly equal fraction of each impurity in each of the samples.

AVERAGE CROSS SECTIONS AND STATISTICAL MODEL FITS

As mentioned earlier the enriched osmium isotope samples are ten times smaller than typical ones the experimental equipment was designed to measure. Thus the measurements were replicated, with particular attention to background and calibration measurements. It was possible in the second cycle to collect considerably more data for each sample and thereby improve the counting statistics. The two sets of runs were combined for each isotope and Figs. 2–5 present the resulting average capture cross sections of ^{186}Os, ^{187}Os, and ^{188}Os. Note that even though each averaging interval includes tens of resonances, nuclear level fluctuations are still apparent even above 50 keV. The errors shown are only those associated with counting statistics and the corrections discussed above and do not include any systematic error es-

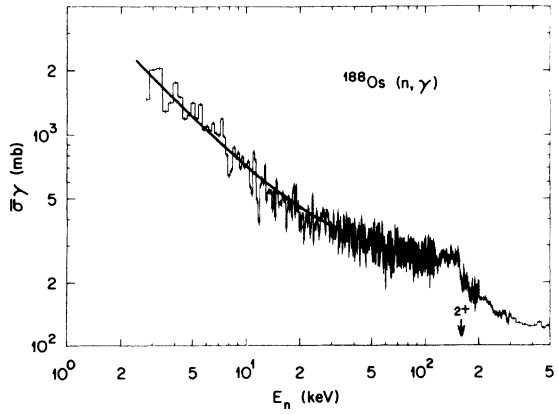

FIG. 2. Effective cross section for ^{186}Os(n,γ). The curve is a statistical model fit to the data below 112 keV. The arrow marks the position of the 2$^+$ first excited state 137 keV above ground. Note the marked effect of the opening of the inelastic channel.

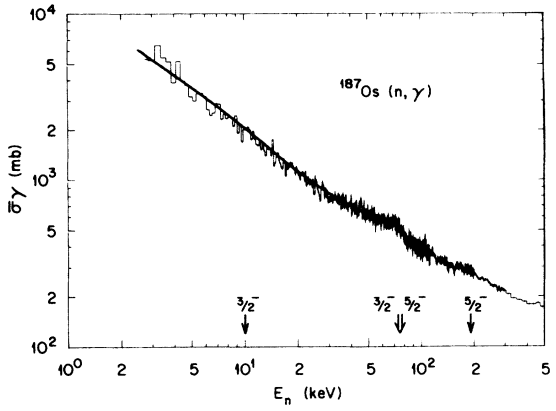

FIG. 3. Effective cross section for ^{187}Os(n,γ). The curve is a statistical model fit to the data below 74 keV. The arrow marks the location of four of the first five excited levels. A $\frac{7}{2}^-$ level at 100.7 keV is not shown. Note that evidence of inelastic competition effects for the 9.75-keV $\frac{3}{2}^-$ state is not obvious but such effects are observed for the 3 higher states.

timates such as uncertainties in the ^{6}Li(n,α) monitor efficiency as a function of energy. The ^{6}Li glass efficiency was determined to (1–2)% relative to the current ENDF/B V ^{6}Li(n,α) and ^{235}U(n,f) cross section standards.[19] A comparison of the first and second runs on each sample allows an estimate of the otherwise unrecognized experimental errors, calculated via the chi square statistic, as a function of energy;

$$\chi^2 = \sum_i (R_i - 1)^2 / V(R_i), \quad i = 186, 187, 188 \qquad (3)$$

R_i is the ratio of the two estimates of the average cross section for the ith isotope. The variance

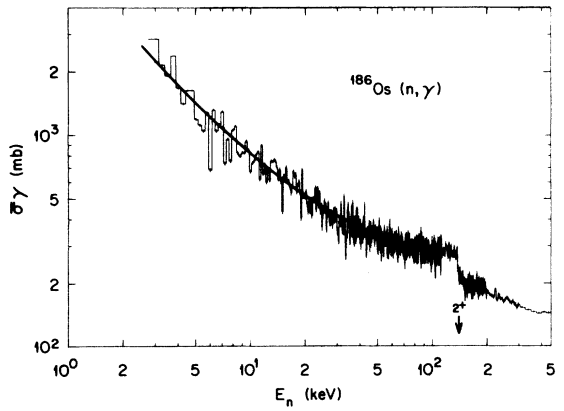

FIG. 4. Effective cross section for ^{188}Os(n,γ). The curve is a statistical model fit to the data below 112 keV. The arrow marks the location of the 2^+ first excited state at 155 keV. Note the competition effects as the inelastic channel opens.

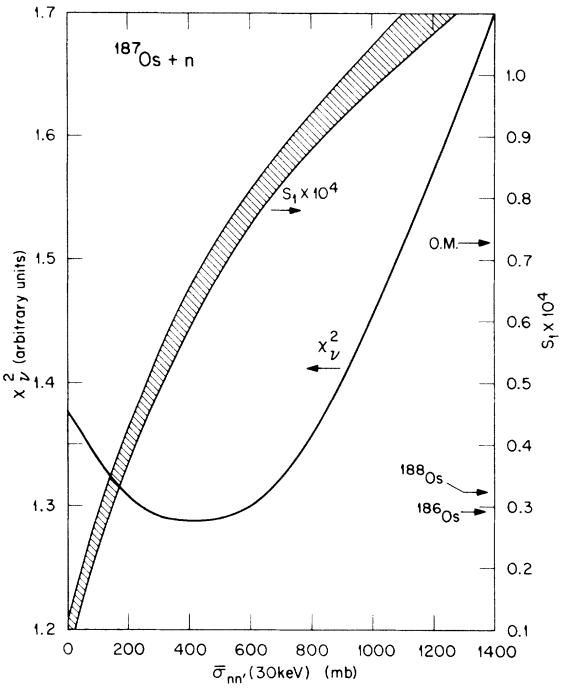

FIG. 5. Quality of the statistical model fit to the ^{187}Os(n,γ) cross section data for various values of the 30-keV inelastic parameter $S_{nn'}$. The corresponding values of S_1 from the fits are shown. The arrows indicate the value of S_1 found for ^{186}Os and ^{188}Os and the result of an optical model calculation (Ref. 16).

$V(R_i)$ of the ratio is calculated in the usual manner for a ratio of two quantities with variances $V[\bar{\sigma}_{\gamma i}(\text{early, late})]$ and where it is assumed that all components of the variances $V[\bar{\sigma}_{\gamma i}]$ are uncorrelated except for the time-dependent, sample-independent backgrounds (determined by scaling the same background) which are assumed to be 100% correlated. An estimate of the "external" error, i.e., including systematic effects, is then obtained from

$$V^e(R_i) = \chi_\nu^2 \, V(R_i), \quad (\text{for } \chi_\nu^2 > 1), \quad i = 186, 187, 188 . \qquad (4)$$

This variance analysis increases the errors of the combined data shown in Figs. 2–5 by a factor of $(\chi_\nu^2)^{1/2} = 4.6$ near 2.5 keV, decreasing to unity at about 20 keV (for $\chi_\nu^2 < 1$, the statistical errors are left unchanged). Thus above ≈20 keV, the uncertainties shown in Figs. 2–5 include *both* measured cross sections for each isotope.

STRENGTH FUNCTIONS AND THE STATISTICAL MODEL OF NEUTRON CAPTURE

The curves shown in Figs. 2–5 are least square fits[20] to the statistical model form of the average

capture cross section,

$$\bar{\sigma}_\gamma(E) = \frac{2\Pi^2}{k^2} \sum_{J^\pi, s} \frac{g(J)\bar{\Gamma}_n(J^\pi)\bar{\Gamma}_\gamma}{D(J^\pi)(\bar{\Gamma}_n(J^\pi))+\bar{\Gamma}_\gamma} F(\bar{\Gamma}_\gamma/\bar{\Gamma}_n(J^\pi)) , \quad (5)$$

where s is the channel spin and where the average neutron width can be written

$$\bar{\Gamma}_n(J^\pi) = S_l \sqrt{E/E_r}\, v_l D(J^\pi) . \quad (6)$$

The reference energy E_r is conventionally taken as 1 eV and the v_l are measures of the probability of a neutron with angular momentum l penetrating the centrifugal barrier. The S_l are the neutron strength functions and $D(J^\pi)$ are the mean spacings for levels of angular momentum J and parity π. In fitting this form to the data, terms for $l=0, 1, 2$ partial waves only were included. Further it is assumed that the average radiative width $\bar{\Gamma}_\gamma$ is independent of spin and parity and that the level densities are $(2J+1)$ dependent. The level fluctuation correction factor $F(\bar{\Gamma}_\gamma/\bar{\Gamma}_n)$ is taken from the work by Lane and Lynn.[21] The lowest excited states in ^{186}Os + n and ^{188}Os + n are at 137 and 155 keV, respectively, and hence the statistical model fits were restricted to the data below 113 keV in order to avoid competition effects as the inelastic channel opens. In the case of ^{187}Os(n,γ), competition effects above the 9.75-keV first excited state (up to the 74- and 75-keV excited states) were incorporated into the statistical model. The model restricts the competition to involve only the $J^\pi = 1^-$ channels (s-wave incident) since the penetrabilities for inelastically scattered neutrons for partial waves greater than $l=0$ are negligibly small. The competition effects in the capture channel ($J^\pi = 1^-$) are assumed to have the form

$$\bar{\sigma}'_\gamma(1^-;E_n) = \bar{\sigma}_\gamma(1^-;E_n) \frac{\bar{\sigma}_\gamma(1^-;E_n)}{\bar{\sigma}_\gamma(1^-;E_n)+\bar{\sigma}_{nn'}(E_n)} , \quad (7)$$

where $\bar{\sigma}_\gamma(1^-;E_n)$ is calculated using the $J^\pi = 1^-$ term in Eq. (5) and

$$\bar{\sigma}_{nn'}(E_n) = C_{nn'} \frac{P_0(E_n)P_0(E_n - E_{th})}{k^2(E_n)R^2} , \quad (8)$$

where P_0 is the penetrability for s-wave neutrons, R is the channel radius, and E_{th} is the threshold for scattering to the first excited state and $C_{nn'}$ varies only slowly with energy (for $E_n > E_{th}$). For convenience and clarity we report $\bar{\sigma}_{nn'}$ (30 keV) $\equiv S_{nn'}$ rather than $C_{nn'}$. This prescription has given excellent descriptions of the competition effects in the case of ^{232}Th(n,γ) (Ref. 22) and ^{159}Tb(n,γ) (Ref. 23). The least squares fits to the average cross sections yield estimates for some or all of the energy independent strength functions S_0, S_1, S_2, and a radiative strength function $S_\gamma = \Gamma_\gamma/D_0$, where D_0 is a mean spacing such that $D(J^\pi) = D_0/(2J+1)$. The value of S_0 was fixed at a common value $S_0 = 2.2\times10^{-4}$ for all three isotopes as the capture data were relatively insensitive to it. This value is consistent both with systematic evaluations[16] and osmium data reported by Vertebnyi.[15] Table III presents the results of these least squares fits. The p-wave strength functions for the ^{186}Os and ^{188}Os are in good agreement with p-wave strength functions reported for the[24,25] tungsten isotopes and suggest that the minimum in the p-wave strength function near mass 180 is significantly deeper than indicated by the optical model fit of Mughabghab.[16] Figure 5 shows the quality of fits (as measured by χ_ν^2) and corresponding values for S_1 for a series of least squares fits using various assumed values for $S_{nn'}$. It is clear from the figure that if the value of S_1 is required to be not more than a factor of 2 different from the values for 186 and 188 and if only fits with χ_ν^2 close to the minimum are accepted, then $S_{nn'} = 0.25(20)$ b and $S_1 \cong 0.45\times10^{-4}$ are acceptable choices. This value for $S_{nn'}$ can be interpreted (since the competition was with the capture only) as a crude lower bound on the inelastic cross section near 30 keV. This bound is consistent with the results of a recent Hauser-Feshbach calculation by Woosley[26] giving 0.8 b for this cross section at 30 keV.

The gamma ray strength functions lead to estimates for average radiative widths (see Table III for D_0) $\bar{\Gamma}_\gamma = 80$ meV (186), 78 meV (187), and 69 meV (188). These are somewhat smaller than

TABLE III. Strength functions from statistical model least squares fits.

Isotope	$S_0\times10^4$	$S_1\times10^4$	$S_2\times10^4$	$S_\gamma\times10^4$	D_0 (eV)
186	2.2 [a]	0.29(2)	1.3(1)	26.8(5)	30 [c]
187	2.2 [a]	0.45 [b]	4.0(1)	176(3)	4.42(17) [d]
188	2.2 [a]	0.33(2)	1.5(1)	20.8(4)	33 [c]

[a] Not varied.
[b] For $S_{nn'} = 0.250$ b, see text for discussion.
[c] Reference 15.
[d] Reference 17.

Vertebnyi's[15] results $\overline{\Gamma}_\gamma = 122(10)$ meV for two resonances in ^{186}Os + n, $\overline{\Gamma}_\gamma = 92(10)$ meV for three resonances in ^{187}Os + n, and $\overline{\Gamma}_\gamma = 110(20)$ meV for one ^{188}Os + n resonance.

The only previously reported measurements of Os capture cross sections in the kilovolt incident neutron energy range are those reported for ^{186}Os(n,γ) and ^{187}Os(n,γ) by Browne and Berman.[5] In Table IV are presented for comparison values of the cross sections (averaged as in Ref. 5) from this work and those taken from Fig. 3 of Ref. 5. The two measurements of the ^{187}Os cross section are in good agreement up to 150 keV, the upper end of Browne's energy range. The ^{186}Os measurements, however, are in substantial disagreement, the cross section from this work ranging from 80% larger at 5 keV and 50% larger at 10 keV, to ~30% larger from 20 to 150 keV. We understand[18] that significant revision of the background corrections primarily affecting the ^{186}Os(n,γ) cross section reported in Ref. 5 removes this discrepancy.

Also presented in Table IV are the results of Hauser-Feshbach statistical model calculations by Holmes *et al.*[27] as modified by Woosley and Fowler[4] to include the measured level spacings and to take nuclear level width fluctuations into account. The calculations overestimate, relative to either set of measurements, both cross sections, although the calculations are in better agreement in shape and normalization with the results of this work. Some adjustment of the nuclear potential and level density parameters used in the Hauser-Feshbach calculations are required to fit the observed capture cross sections. Such improvement would also be expected to enhance the accuracy of Woosley's calculation of the inelastic cross section and its effects on capture.

MAXWELLIAN-AVERAGED CROSS SECTIONS

Since s-process heavy element nucleosynthesis is assumed[28] to take place in stellar interiors, the neutrons and nuclei are expected to obey a Maxwell-Boltzman energy distribution. Hence, it is the Maxwellian-averaged capture cross sections $\langle\sigma_\gamma\rangle \equiv \langle\sigma_\gamma v\rangle / v_T$ which are of importance in astrophysics. The Maxwellian-averaged osmium 186, 187, and 188 capture cross sections are shown in Fig. 6 for a range of temperatures (kT) characteristic of stellar interiors. There was only one significant departure from the Maxwellian-averaging procedure as described by Allen *et al.*[29] The statistical model fits [Eq. (7) and Table III] were used below $E_n = 2.5$ keV, the lower limit of our data. The error estimates were obtained by propagating the cross section variance estimates (including the systematic effects discussed above) through the Maxwellian averaging assuming all components of the variance to be uncorrelated. The assumed (50%) uncertainty in the s-wave strength functions dominates the error estimates up to $kT \approx 30$ keV even though the strength function contribution at 30 keV is only $\simeq 4\%$.

The ORELA 30 keV Maxwellian cross sections for ^{186}Os and ^{187}Os are rather close to the semi-empirical estimates made by Allen *et al.*,[29] 0.330 b (cf. 0.467 b, this work) for ^{186}Os and 0.900 b (cf. 0.927 b) for ^{187}Os. The odd-A/even-A capture cross section ratio we find near 30 keV is only 10% lower than the empirical average (2.2) reported by Macklin[30] for many elements and sometimes used (e.g., Allen[29]) to predict unmeasured cross sections.

TABLE IV. Comparison of Os(n,γ) cross sections from this work with the work by Browne and Berman[c] and Hauser-Feshbach calculations by Holmes *et al.*[d] as modified in Ref. 4.

E_n (keV)	$\overline{\sigma}_\gamma$(186) b This work	Browne *et al.*[c]	H-F[d,e]	$\overline{\sigma}_\gamma$(187) b This work	Browne *et al.*[c]	H-F[d,e]
5	1.37[a]	0.76[b]	1.37	3.54[a]	3.2[b]	3.50
10	0.83	0.55	0.95	2.06	1.9	2.34
20	0.52	0.44	0.68	1.14	1.1	1.34
30	0.41	0.33	0.57	0.82	0.85	1.08
50	0.33	0.27	0.45	0.63	0.64	0.81
100	0.27	0.21	0.37	0.39	0.36	0.46
150	0.20	0.15	0.26	0.25	0.34	0.31

[a] Uncertainty in these numbers $\lesssim 2\%$, dominated by the uncertainties in the flux monitor normalization.

[b] Reference 5 gives an estimate of uncertainty of 8% for these entries.

[c] Reference 5. See text, however, for revision to 186 (Col. 3).

[d] Reference 27.

[e] Reference 4.

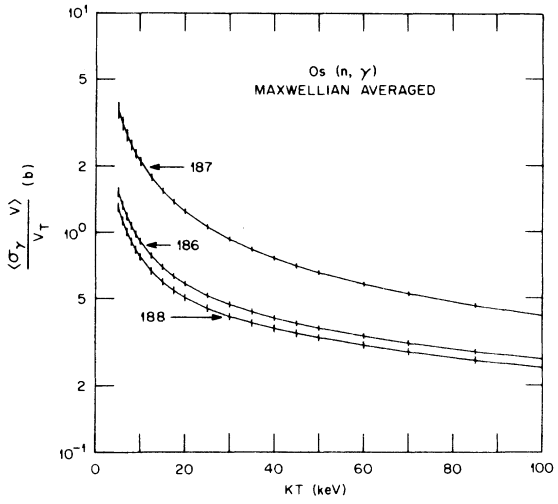

FIG. 6. The Maxwellian-averaged capture cross section $\langle \sigma_\gamma \rangle$ for the osmium isotopes 186, 187, and 188. The error bars shown include the systematic errors discussed in the text.

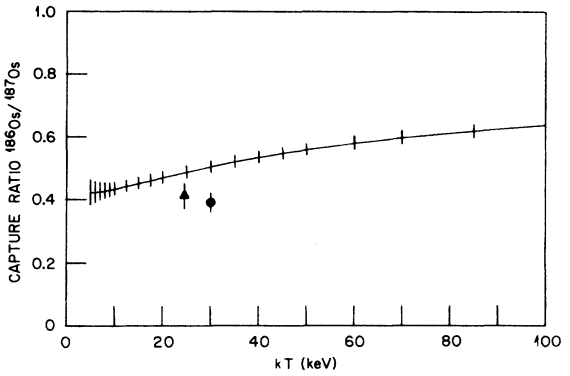

FIG. 7. The ratio $\langle \sigma_\gamma(186) \rangle / \langle \sigma_\gamma(187) \rangle$ as a function of kT for stellar temperatures. The triangle shows the result of a measurement at the NBS (Ref. 6) and the circle, a measurement at LLL (Ref. 5). See text for revisions of both the NBS and LLL results.

$\langle \sigma_\gamma(186) \rangle / \langle \sigma_\gamma(187) \rangle$

An important parameter required by the Re-Os cosmochronometer is the ratio of ^{186}Os to ^{187}Os Maxwellian-averaged cross sections. We find $\langle \sigma_\gamma(186) \rangle / \langle \sigma_\gamma(187) \rangle = 0.504(17)$ at $kT = 30$ keV. The ratio as a function of kT in the range of astrophysical interest is shown in Fig. 7 and listed in Table V. The variance analysis for the ratios assumed all components of the variances of the cross sections to be uncorrelated except for those components associated with the time-dependent, sample-independent background corrections. These were taken as fully correlated since the same background determination was scaled to correct all six cross section measurements. Also shown in Fig. 7 are the only two previously reported measurements of this ratio. The measurement 0.41(4) near 24.5 keV by Browne *et al.*[6] was made at the National Bureau of Standards (NBS) 10 – MW reactor using an iron-filtered neutron beam. For comparison with the NBS result, the cross sections from our work were averaged using a Gaussian weighting function with FWHM = 3.7 keV, the value reported[6] as the width of the iron window. The resulting ratio of cross sections is 0.49(1), significantly larger than the NBS result. The NBS reactor beam experiments consisted of several runs having high and variable backgrounds. The two best runs (lowest background) gave[18] 0.46 and 0.49 for the ratio, in much better agreement with our results. Our result at 30 keV is likewise significantly larger than Browne and Berman's[5] result 0.39(3) (see Fig. 7) from an experiment at the Lawrence Livermore (LLL) 100 MeV Linac. The revision,[18] discussed above, gives a ratio 0.49(4) in excellent agreement with us.

TABLE V. ^{186}Os, ^{187}Os, and ^{188}Os Maxwellian-averaged capture cross sections for various temperatures (T). The error estimates shown include the systematic effects discussed in the text.

kT (keV)	$\langle \sigma_\gamma(186) \rangle$ b	$\langle \sigma_\gamma(187) \rangle$ b	$\langle \sigma_\gamma(188) \rangle$ b	$\frac{\langle \sigma_\gamma(186) \rangle}{\langle \sigma_\gamma(187) \rangle}$
10	0.907(28)	2.09(9)	0.770(29)	0.434(23)
20	0.581(15)	1.24(3)	0.503(18)	0.469(17)
30	0.467(12)	0.927(19)	0.413(15)	0.504(17)
50	0.365(9)	0.654(13)	0.331(11)	0.559(18)
100	0.266(7)	0.418(9)	0.242(8)	0.636(21)

AGE OF THE ELEMENTS

The use of the ^{187}Re → ^{187}Os beta decay as a measure of the duration of nucleosynthesis Δ has received considerable attention since the possibility was first suggested by Clayton[1] some fifteen years ago. Discussions of the use of the Re-Os decay as a nucleosynthetic chronometer can be found (among other sources) in Clayton's original paper,[1] a text by Clayton,[28] and in an article by Fowler.[31] Three features of the Re → Os decay make it appear uniquely well suited as a chronometer of heavy-element nucleosynthesis (see Fig. 8). (1) ^{187}Re can be made only by the r process since the s-process path follows the ^{186}Re β decay to ^{186}Os. The 91 hour ^{186}Re decay half-life is very much shorter than the s-process mean neutron capture time.[32] (2) The stable isotope ^{186}W shields ^{186}Os from the r process and hence the abundance of ^{186}Os is entirely due to the s process. (3) The abundance of ^{187}Os

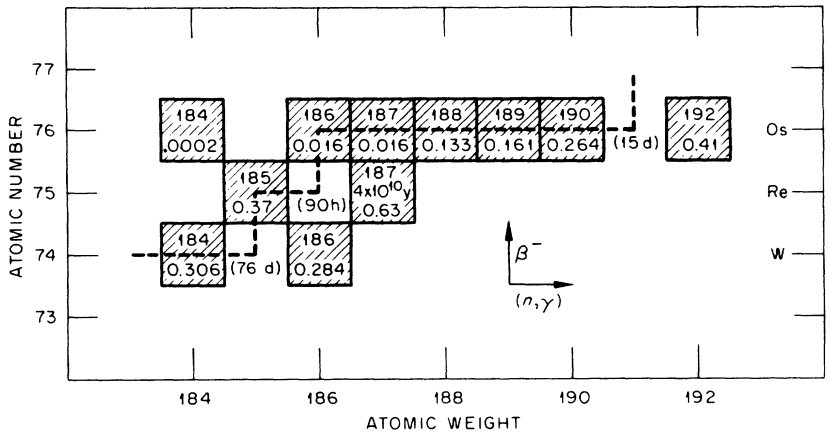

FIG. 8. The path of the s process of nucleosynthesis in the region involving Re and Os. Note that ^{186}Os and ^{187}Os are shielded from the r process.

is due to both the s process through ^{186}Os and to the beta decay of ^{187}Re. Thus if the s-process osmium-187 abundance ^{187}Os(s) (the chemical symbol will be used to represent abundances) is subtracted from the primordial total osmium-187 abundance ^{187}Os, the difference ^{187}Os(β) is attibuted to the ^{187}Re beta decay and is a measure of the duration of nucleosynthesis. Clayton's[1] local approximation can be used to calculate ^{187}Os(s),

$$^{187}\mathrm{Os}(s) = {}^{186}\mathrm{Os}\langle\sigma_\gamma^*(186)\rangle/\langle\sigma_\gamma^*(187)\rangle \qquad (9)$$

since ^{186}Os(s) = ^{186}Os. The symbol σ_γ^* represents the neutron capture cross section at *steller temperatures*. Holmes *et al.*[27] show that these stellar cross sections can be obtained from the laboratory cross sections $\langle\sigma_\gamma\rangle$ by multiplication by an enhancement factor $f \equiv \langle\sigma_\gamma^*\rangle/\langle\sigma_\gamma\rangle$. They also present the results of Hauser-Feshbach calculations of what appear to be the best estimates of the cross section enhancement factors f due to population of nuclear excited states. They report for the $kT = 30$ keV cross section for ^{186}Os, $f = 1.01$ and for ^{187}Os, $f = 1.23$. Hence, the 186/187 cross section ratio as measured in the laboratory should be "enhanced" by a factor $F_{67} = 0.83$. At least two less precise estimates of F_{67} larger than unity have been published.[4,33] This, plus the fact that the Hauser-Feshbach calculated ^{186}Os capture cross section is in disagreement with the measurement, suggest a substantial uncertainty in F_{67} and hence in the estimate of ^{187}Os(s). For this work $F_{67} = 0.83$ is adopted as the best estimate currently available (see Ref. 4 for more nearly complete discussions of the consequences of the uncertainty in F_{67}).

Thus, the ratio of ^{187}Os(β) to the parent ^{187}Re can be written,[1]

$$\frac{^{187}\mathrm{Os}(\beta)}{^{187}\mathrm{Re}} = \frac{(^{187}\mathrm{Os}/\mathrm{Os}) - F_{67}(^{186}\mathrm{Os}/\mathrm{Os})\langle\sigma_\gamma(186)\rangle/\langle\sigma_\gamma(187)\rangle}{(^{187}\mathrm{Re}/\mathrm{Re})}\,\frac{\mathrm{Os}}{\mathrm{Re}} \qquad (10)$$

The abundance ratios[34] appearing in Eq. (10) used in this work are given in Table VI. The primordial, i.e., at time Δ after r-process nucleosynthesis begins, ratio appearing on the left-hand side of Eq. (10) can also be written,[1] in terms of an exponential model for r-process nucleosynthesis, as

$$\frac{^{187}\mathrm{Os}(\beta)}{^{187}\mathrm{Re}} = \frac{\lambda_R - \lambda_\beta}{\lambda_R}\,\frac{1 - \exp(-\lambda_R\Delta)}{\exp(-\lambda_\beta\Delta) - \exp(-\lambda_R\Delta)} - 1, \qquad (11)$$

$\lambda_\beta = \ln 2/\tau_\beta$, where λ_β is the ^{187}Re-^{187}Os mean beta decay rate. Discussions of measurements of τ_β and the associated uncertainties are given in Refs. 35–37. The effects of temperature in the stellar environment on τ_β are discussed in Refs. 2–4. A perusal of these references reveals considerable uncertainty concerning the value of τ_β. We adopt $\tau_\beta = 44\times10^9$ yr, a value in reasonable ($\approx$20%) agreement with the result from what appears to be the best β counting measurement[36] and the result deriving from rock-dating techniques (see for example Refs. 31 and 38).

Clearly a choice has to be made from a range of exponential models from a uniform rate ($\lambda_R = 0$) of r-process nucleosynthesis to a sudden ($\lambda_R \to \infty$) r-process nucleosynthetic event. Fowler[31] suggested an intermediate model such that the r-

TABLE VI. Meteoritic abundance data used in Eq. (10) of the text.

	Present[a]	Primordial
$^{186}Os/Os$	0.0159[a]	0.0159
$^{187}Os/Os$	0.0164[a]	0.0125(4)[c]
$^{187}Re/Re$	0.63[a]	0.65[c]
Os/Re	13.8(6)[b]	13.1(10)[c]

[a] See Ref. 34 for additional references.
[b] From *C*1 chrondrites, Ref. 34.
[c] Calculated using $\tau_\beta = 4.4 \times 10^{10}$ yr (Refs. 35–37). The error quoted does not include the uncertainty in τ_β.

process rate at the time of solar system formation is 9% of the initial rate, i.e., $\lambda_R \Delta = \frac{1}{0.43}$. Adopting that choice, Fig. 9 presents the results of simultaneously solving Eqs. (10) and (11) for Δ. The ORELA result for the cross section ratio 0.504(17) leads to Δ = 10.4(4) billion years. The uncertainty estimate (shown as *solid* error bars in Fig. 9) reflects *only* the uncertainty in the cross section ratio. If a 20% uncertainty in the half-life τ_β is assumed and the other uncertainties shown in Table VI are included, the uncertainty in the value for Δ becomes 2.5 billion years. Clearly this is only approximately correct since the uncertainty in τ_β could be much larger than 20%. This uncertainty estimate for Δ is shown in *dashed* error bars in Fig. 9. Thus, using the ORELA cross section ratio, the Re-Os chronometer yields 10.4(25) billion years for Δ. This result is consistent with the estimate (using the same exponential model) Δ = 7(2) billion years from U/Th (see Fig. 9). The published (unrevised) Livermore ratio (also shown in Fig. 9) leads to Δ = 12.9(30) billion years, not quite consistent with the U/Th result. With their[18] revision discussed above, that apparent disagreement is removed. It seems clear that uncertainties in the cross section ratio are no longer the major problem in use of the Re-Os chronometer.

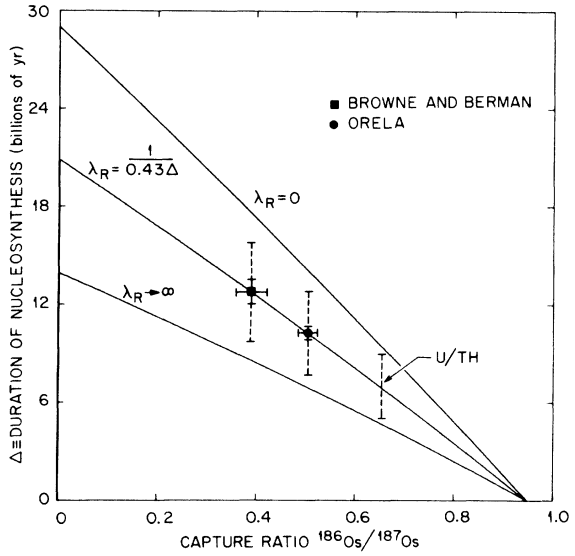

FIG. 9. The ^{187}Re-^{187}Os chronometer. The square is the result of the LLL measurement (Ref. 5) (without revision, see text) and the circle, the result from this work. The estimate for the duration of galactic nucleosynthesis derived from this work, $10.4(25) \times 10^9$ is consistent with the estimate using U/Th, 7.0(20). The characteristic *r*-process rate factor 0.43 (and the U/Th age) is adopted from model parameters (Ref. 31) based on ^{244}Pu and ^{124}I abundances of Wasserburg *et al.* Other sets of model parameters suggested to us lead to slightly greater ages, still within the error bars shown.

r-PROCESS ABUNDANCE OF ^{188}Os

The local *s*-process approximation applied to $^{186}Os(s)$ and $^{188}Os(s)$ [through $^{187}Os(s)$], allows us to also calculate the primordial *r*-process contribution to the osmium-188 abundance, in terms of ^{186}Os and the enhanced ratio $F_{68}\langle\sigma_\gamma(186)\rangle / \langle\sigma_\gamma(188)\rangle$. The stellar temperature enhancement factor $F_{68} = 1.007$ is taken from Holmes *et al.*[27] We find $^{188}Os(r) = 0.083$ (on the $Si = 10^6$ scale of abundances), which compared to $^{187}Re = 0.036$ ($Si = 10^6$) from the above provides an example of the important odd/even fluctuations expected in the *r*-process abundances.

CONCLUSION

Remeasurement of the $^{186,187,188}Os$ neutron capture cross sections has reduced the discrepancy between calculations of the age of the galaxy prior to solar condensation as determined by the Re-Os and the U/Th chronologies. The average nuclear parameters we find are in reasonably good agreement with compound nucleus calculations and with nuclear systematics.

ACKNOWLEDGMENTS

The authors are grateful to G. Rogosa for help in obtaining the enriched osmium samples. One of the authors (RRW) expresses his appreciation to the U. S. Department of Energy for partially funding the sabbatical leave during which this work was done. The research was sponsored by the Division of Nuclear Sciences, U. S. Department of Energy, under Contract No. W-7405-eng-26 with the Union Carbide Corporation.

*Permanent address: Denison University, Granville, Ohio.
[1]D. D. Clayton, Ap. J. 139, 637 (1964).
[2]J. Conrad and H. D. Zeh, Z. Naturforsch. (to be published).
[3]R. J. Talbot, Jr., Astrophys. Space Sci. 20, 241 (1973).
[4]S. E. Woosley and W. A. Fowler, Ap. J. (to be published).
[5]J. Browne and B. Berman, Nature 262, 197 (1976).
[6]J. Browne, G. P. Lamaze, and I. G. Schroder, Phys. Rev. C 14, 1287 (1976).
[7]See B. J. Allen *et al.*, Phys. Rev. C 8, 1504 (1973) and R. L. Macklin and R. R. Winters, Phys. Rev. C 7, 1966 (1973) for further references describing the capture facility.
[8]H. Maier-Leibnitz, Oak Ridge National Laboratory, report, 1963 (unpublished)
[9]R. L. Macklin, J. Halperin, and R. R. Winters, Phys. Rev. C 11, 1270 (1975).
[10]N. Yamamuro *et al.*, Nucl. Instrum. Methods 133, 531 (1976).
[11]R. L. Macklin, J. Halperin, and R. R. Winters, Nucl. Instrum. Methods (to be published).
[12]R. L. Macklin, Nucl. Sci. Eng. 59, 12 (1976).
[13]R. L. Macklin, Nucl. Instrum. Methods 26, 213 (1964).
[14]L. Dresner, Nucl. Instrum. Methods 16, 176 (1962).
[15]V. P. Vertebnyi *et al.*, Yad. Fiz. 22, 674 (1975) [Sov. J. Nucl. Phys. 22, 348 (1975)].
[16]S. F. Mughabghab and D. I. Garber, Report No. BNL-325, 3rd ed., I, 1973 (unpublished).
[17]A. Stolovy, A. I. Namenson, and B. L. Berman, Phys. Rev. C 14, 965 (1976).
[18]J. Browne (private communication).
[19]R. L. Macklin, R. W. Ingle, and J. Halperin, Nucl. Sci. Eng. 71, 182 (1979).
[20]M. Mizumoto, R. L. Macklin, and J. Halperin, Phys. Rev. C 17, 522 (1978).
[21]A. M. Lane and J. E. Lynn, Proc. Phys. Soc. London A70, 557 (1957).
[22]R. L. Macklin and J. Halperin, Nucl. Sci. Eng. 64, 849 (1977).
[23]M. Mizumoto, R. L. Macklin, and J. Halperin, Phys. Rev. C 17, 522 (1978).
[24]H. S. Camarda, Columbia University Report No. 293 (unpublished).
[25]Z. M. Bartholome, R. W. Hockenbury, W. R. Moyer, J. R. Tatarczuk, and R. C. Block, Nucl. Sci. Eng. 37, 137 (1969).
[26]S. Woosley (private communication).
[27]J. A. Holmes, S. E. Woosley, W. A. Fowler, and B. A. Zimmerman, At. Data Nucl. Data Tables 18, No. 4 (1976).
[28]D. D. Clayton, *Principles of Stellar Evolution and Nucleosynthesis* (McGraw-Hill, New York, 1968).
[29]B. A. Allen, J. H. Gibbons, and R. L. Macklin, in *Advances in Nuclear Physics 4*, edited by E. Vogt (Plenum, New York, 1971).
[30]R. L. Macklin, J. H. Gibbons, and T. Inada, Phys. Rev. 129, 2695 (1963).
[31]W. A. Fowler, in *Cosmology Fusion and other Matters*, edited by F. Reines (Colorado State University Press, Fort Collins, 1972).
[32]R. L. Macklin and R. R. Winters, Astrophys. J. 208, 812 (1976).
[33]W. A. Fowler, in *Explosive Nucleosynthesis*, edited by D. N. Schramm and W. D. Arnett (University of Texas Press, Austin, 1973).
[34]J. W. Morgan, *Handbook of Elemental Abundances in Meteorities*, edited by B. Mason (Gordon and Breach, New York, 1972).
[35]R. L. Brodzinski and D. C. Conway, Phys. Rev. B 138, 1368 (1965). See this reference for a summary of earlier work.
[36]J. A. Payne and R. Drever, Ph.D. dissertation, University of Glascow, 1965 (unpublished).
[37]B. Hirt *et al.*, *Earth Science and Meteorites*, edited by J. Geiss and E. D. Goldberg (North-Holland, Amsterdam, 1963).

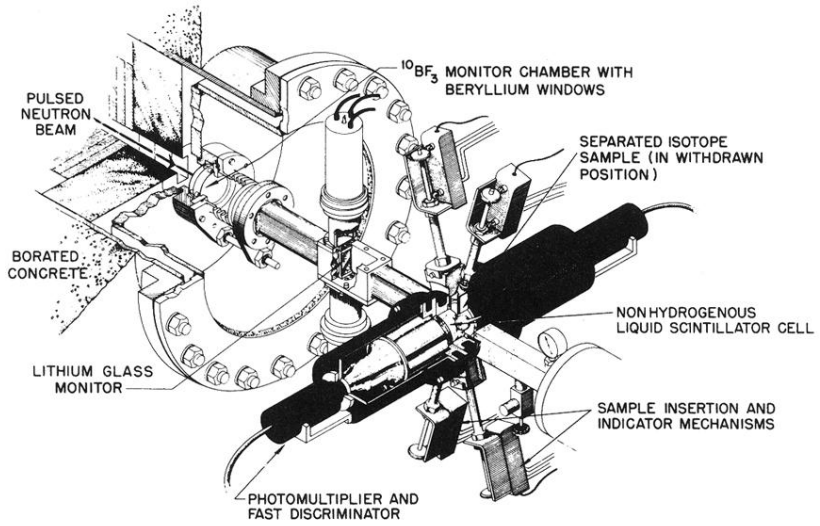

FIG. 1. The ORELA capture facility on flight path 7 at the 40 m flight path station.